

Inversion of specific heat oscillations with in-plane magnetic field angle in 2D d -wave superconductors

G. R. Boyd,¹ P. J. Hirschfeld,¹ I. Vekhter,² and A. B. Vorontsov^{2,*}

¹*Department of Physics, University of Florida, Gainesville, FL 32611, USA*

²*Department of Physics and Astronomy, Louisiana State University, Baton Rouge, Louisiana 70803 USA*

Experiments on several novel superconducting compounds have observed oscillations of the specific heat when an applied magnetic field is rotated with respect to the crystal axes. The results are commonly interpreted as arising from the nodes of an unconventional order parameter, but the identifications of nodal directions are sometimes controversial. Here we show with a semiclassical model calculation that when the magnetic field points in the direction of the nodes, either minima or maxima can occur in the specific heat depending on the the temperature T and the magnetic field H . An inversion of the angular oscillations takes place with respect to those predicted earlier at low temperature by the nodal approximation. This result, together with the argument that the inversion takes place based on an approximation valid at moderate fields, indicates that the inversion of specific heat oscillations is an intrinsic feature of nodal superconductors.

PACS numbers:

I. INTRODUCTION

Initial information on the symmetry of the order parameter in newly discovered superconductors is often provided by power laws in the temperature dependence of thermodynamic and transport properties¹. However, the exact nodal structure cannot be determined by these techniques because the same exponents may correspond to order parameters with different symmetries. Phase-sensitive experiments like the tricrystal experiments performed on cuprates² are the most definitive, but are technically challenging and require high quality samples. A simpler technique, proposed in Ref. 3, which is not phase sensitive, but provides information on the distribution of nodes on the Fermi surface, is a measurement of the specific heat in the presence of a magnetic field, \mathbf{H} , which is rotated with respect to the crystal axes of the sample. It was shown in that work that, if the effect of the superflow due to vortices on the quasiparticle spectrum was treated semiclassically, via the Doppler energy shift^{4,5}, the low-temperature specific heat of a superconductor with line nodes acquires an oscillatory dependence on the field orientation. In particular, the low-temperature specific heat coefficient $\gamma \sim T\sqrt{H}$ was shown to have minima when the magnetic field points in the direction of the nodes in the order parameter, and maxima for the field along the antinodes, where the gap is maximal. Ref. 3 and its extension, Ref. 6 made use of two additional approximations. First, they replaced the Doppler energy shift of a quasiparticle with momentum \mathbf{k} near one of the nodes by its value at the node, $\mathbf{k} = \mathbf{k}_n$. This so-called nodal approximation had been shown to work well compared to the full semiclassical evaluation in Ref. 5, providing $T, E_H \ll \Delta_0$. Here Δ_0 is the maximum gap over the Fermi surface, and $E_H \sim \Delta_0\sqrt{H/H_{c2}}$, where H_{c2} is the upper critical field, is a magnetic energy scale (see Sec. II). Second, making predictions for low temperatures and fields, $T, E_H \ll \Delta_0$, the authors of Refs.^{3,6} used a form

of the order parameter linearized in the vicinity of the nodal points.

By now there have been several experimental tests of these ideas⁷⁻¹³, and the observations have been generally consistent with theoretical expectations. At the same time, the assignment of the nodal directions in several materials remains controversial. In CeCoIn₅ the measurements of the anisotropy of the specific heat⁹ and the thermal conductivity^{14,15} appear to give contradictory results for the gap structure. In Sr₂RuO₄ the specific heat oscillations were observed to *invert* as the temperature and field was varied, i.e. the minima and maxima as a function of angle changed places^{10,13}.

Such an inversion was never found in earlier theoretical calculations within the semiclassical approach, even though it was found in theoretical work employing other techniques, see below. This clearly poses a problem: if the technique is to be useful as a way to “map” out the nodal structure, it is necessary to be able to predict if and when such inversions will occur; otherwise the nodes in the order parameter may be assigned to incorrect locations in momentum space.

Numerical solution of the Bogoliubov-deGennes equations yielded an inversion in the anisotropy of the density of states (DOS), $N(\omega, \theta)$, between the field applied in the nodal and antinodal directions¹⁶, but this was argued to reduce, rather than invert, the specific heat anisotropy. Recently Vorontsov and Vekhter^{17,18} considered the limit $H_{c1} \ll H \leq H_{c2}$ by extending the method of Brandt, Pesch and Tewordt^{19,20}, and found an agreement with semiclassical method at low T, H , but an inversion of the specific heat oscillations over a large part of the $T - H$ phase diagram. Since the approximation they used was tailored for moderate to high fields, their determination of location (or, indeed, the existence) of the inversion line could be questioned.

In this paper we demonstrate that this inversion is a generic feature of the specific heat in unconventional superconductors. We revisit the semiclassical approach to

the in-plane specific heat oscillations of a quasi-two dimensional d -wave superconductor, but relax the approximations which led in Refs.^{3,6,21} to simple analytical forms for $C(T; \theta)$ at low temperatures. We are thus forced to do a numerically demanding evaluation of the entropy and specific heat, which involves a 2D \mathbf{k} -summation and a 2D averaging over a vortex lattice unit cell. Our model is not restricted to low temperatures, and is valid (within limits discussed below) in the low field regime $H_{c1} \lesssim H \ll H_{c2}$. It may thus be considered to complement the results of Refs.^{17,18}. We find that the anisotropy of the specific heat is inverted as the temperature is increased. This result demonstrates that the inversion phenomenon is robust across the phase diagram for unconventional superconductors, and provides an important caveat to the interpretation of the stationary points in specific heat oscillations.

II. THE SEMICLASSICAL APPROACH

In superconductors with line nodes, the vortex core contribution to the low-energy density of states is smaller than that from the quasiparticles outside the core region⁴. In systems with short coherence length, such as cuprates and heavy fermion materials, the dominance of the extended quasiparticle states is even more pronounced since the spacing of the energy levels in the vortex core is large, and only few such levels (if any exist at all) are occupied at low temperature. Bulk quasiparticles in the vortex state are excited from the pair condensate moving with the superflow around each vortex; hence the effect of applied magnetic field can be simply described by Doppler-shifting the spectrum of extended quasiparticle states according to the local value of the superfluid velocity, $\mathbf{v}_s(\mathbf{r})$. This approximation is valid at $H \ll H_{c2}$, when the vortices are far apart and $\mathbf{v}_s(\mathbf{r})$ varies slowly on the scale of the superconducting coherence length. Using this approach, Volovik predicted⁴ that the density of states at the Fermi level in the vortex state of a superconductor with line nodes varies as $N(\omega = 0; H) \propto \sqrt{H}$. Specific heat measurements on high- T_c cuprates verified the \sqrt{H} field dependence^{22–24}, which played an important role in the identification of d -wave symmetry. It should be noted, however, that the result holds for any gap with line nodes, including, for example, some p -wave states. The \sqrt{H} dependence is modified by the presence of disorder to $H \log H$ as shown by Kübert and Hirschfeld²⁵, but remains nonlinear and qualitatively similar to the pure case.

The semiclassical approximation provides a conceptually transparent and tractable approach to the effect of the vortex lattice on low-lying quasiparticle states. Its validity has been questioned by several authors, who attempted a more accurate description of the effect of both applied field and supercurrents on the quasiparticle spectrum. Franz and Tešanović²⁶ introduced a singular gauge transformation that takes into account both the super-

current distribution and the magnetic field, and mapped the full quantum-mechanical problem onto that of nodal Dirac fermions interacting with effective scalar and vector potentials that are periodic in the unit cell of the vortex lattice. They discovered significant differences from the quasiclassical theory in the quasiparticle excitations at very low energy, as is to be expected since the semiclassical approach works only for large quantum numbers. We do not discuss the details of this breakdown here, since it was done by Knapp et al.^{27,28}, who explicitly compared the quantum-mechanical and semiclassical results for the density of states, and found that small differences between the two approaches begin to appear below a crossover scale which is exponentially small in the Dirac cone anisotropy v_F/v_2 . Here v_F is the Fermi velocity, and $v_2 \equiv d\Delta/dk_{\parallel}$ is the gap “velocity” at the node (k_{\parallel} is the momentum component along the Fermi surface). Since in real materials this ratio is large, and in real samples the presence of impurity scattering and the disorder in the vortex lattice smear out the energy structure on small scales, we assume that for purposes of comparison with the measurements, the semiclassical description is adequate.

Dahm et al.²⁹ investigated in detail the comparison of the simple single vortex Doppler shift approach with the solution of the quasiclassical microscopic Eilenberger equations using several techniques including the Brandt, Pesch, and Tewordt approximation^{19,20}. At distances from the vortex of the order of the coherence length, the Doppler shift method is quantitatively inadequate because of core state contributions or scattering resonances, but these effects have little qualitative impact on the calculation of thermodynamic properties. We therefore proceed with the simplest Doppler-shift analysis for a single vortex unit cell, in order to make the qualitative point which is the main result of this work.

For concreteness, we consider a quasi-two dimensional superconductor with d -wave symmetry. This situation is most closely realized in cuprates, possibly the heavy fermion 115 compounds^{14,30}, and potentially also the newly-discovered oxypnictide materials³¹. We consider the field applied parallel to the conducting plane, $\mathbf{H} \parallel ab$, and assume that the system is sufficiently three-dimensional, so that at the fields of interest the structure of the mixed state resembles the Abrikosov vortex lattice penetrating a stack of weakly coupled 2D planes³². In this case the vortex superflow field \mathbf{v}_s is three dimensional, different on different planes within the vortex unit cell. For weak interlayer coupling we consider a circular in-plane Fermi surface, and therefore account only for quasiparticles with momenta $\mathbf{k} \parallel ab$. Deviations from Fermi surface isotropy and effects of multiple Fermi surface sheets have been studied e.g. in Refs.³³ and³⁴, but do not affect the qualitative conclusions we wish to draw here.

The single-particle Green’s function in the presence of a superflow velocity field \mathbf{v}_s is obtained by Doppler shifting the quasiparticle states with energy ω and momentum

\mathbf{k}^5 (we use units with $\hbar = k_B = 1$),

$$G(\mathbf{k}, \mathbf{r}, \omega_n) = -\frac{(i\omega_n - \mathbf{v}_s(\mathbf{r}) \cdot \mathbf{k})\tau_0 + \Delta_{\mathbf{k}}\tau_1 + \xi_{\mathbf{k}}\tau_3}{(i\omega_n - \mathbf{v}_s(\mathbf{r}) \cdot \mathbf{k})^2 - \xi_{\mathbf{k}}^2 - \Delta_{\mathbf{k}}^2}, \quad (1)$$

where ω_n is the fermionic Matsubara frequency, $\xi_{\mathbf{k}}$ is the band energy measured with respect to the Fermi level, τ_i are Pauli matrices in particle-hole space, and $\Delta_{\mathbf{k}} = \Delta_0 \cos 2\phi$, with ϕ the azimuthal angle on the Fermi surface.

We consider the magnetic field, \mathbf{H} , applied in the ab plane, and approximate the superflow by that of an anisotropic 3D superconductor in the London model. The contours of constant \mathbf{v}_s are then elliptical due to anisotropy of the penetration depth, $\lambda_{ab} \neq \lambda_c$. After rescaling the c -axis by $z' = z\lambda_{ab}/\lambda_c$, the superflow is cylindrically symmetric and the Doppler shift for quasiparticles at the Fermi surface is given by^{3,6}

$$\mathbf{v}_s(\mathbf{r}) \cdot \mathbf{k}_F = \frac{\hbar k_F}{2mr} \sin(\psi) \sin(\theta - \phi), \quad (2)$$

where ψ is the winding angle of the superfluid velocity in real space, θ is the angle between \mathbf{H} and the a -axis, and r is the rescaled distance from the center of the vortex. Note that we explicitly exclude from consideration quasi-1D Fermi surfaces such as those shown by Tanaka et al.³⁴ to lead to $C(H; \theta)$ oscillation inversion at low temperatures.

From Eqs. (1) the local density of states is

$$\begin{aligned} N(\omega, \mathbf{r}) &= -\frac{1}{2\pi} \text{Im} \sum_{\mathbf{k}} \text{Tr} G(\mathbf{k}, \omega - \mathbf{v}_s(\mathbf{r}) \cdot \mathbf{k}) \\ &\simeq N_0 \text{Re} \int_0^{2\pi} \frac{d\phi}{2\pi} \frac{|\omega - \mathbf{v}_s(\mathbf{r}) \cdot \mathbf{k}_F|}{\sqrt{(\omega - \mathbf{v}_s(\mathbf{r}) \cdot \mathbf{k}_F)^2 - |\Delta_0(\phi)|^2}}. \end{aligned} \quad (3)$$

Here N_0 is the normal state density of states. The net DOS per volume is found by spatially averaging $N(\omega, \mathbf{r})$ over a unit cell of the vortex lattice containing one flux quantum, Φ_0 . After rescaling the c -axis the unit cell area increases by a factor λ_c/λ_{ab} , and therefore flux quantization dictates that the quasiparticles now experience the effective field $H^* = (\lambda_{ab}/\lambda_c)H$. In the new coordinates the radius and the area of such a cell are $R_H = \sqrt{\Phi_0/\pi H^*}$ and $A_H = \pi R_H^2$ respectively. Introducing polar coordinates, $\mathbf{r} = R_H(\rho \cos \psi, \rho \sin \psi)$, we find for the average field-dependent density of states

$$N(\omega, \mathbf{H}, T) = \frac{1}{\pi} \int_0^1 \rho d\rho \int_0^{2\pi} d\psi N(\omega, \mathbf{r}). \quad (4)$$

The density of states depends on the angle between the field and the crystal axes. At low energies the dominant contribution to the local DOS is from the near-nodal regions, $\phi \sim \phi_n = \pi/4 \pm n\pi/2$, with $n = 0 \dots 3$, and oscillations in $N(\omega, \mathbf{H}, T)$ appear since the Doppler shift at a given node vanishes when the field is aligned with that node. In the nodal approximation with linearized order parameter, the analytical form of the density of states

was obtained^{3,5,6}, see next Section; however, as pointed out before, this approximation does not give the reversal of the anisotropy (see below).

In all of the following we carry out the full summation over the momenta and the real space coordinates. We use the density of states to compute the entropy,

$$S = -2 \int_{-\infty}^{\infty} d\omega N(\omega) [(1 - f(\omega)) \log(1 - f(\omega)) + f(\omega) \log f(\omega)], \quad (5)$$

where $f(\omega) = (\exp(\omega/T) + 1)^{-1}$ is the Fermi function. To obtain the the heat capacity at constant volume we differentiate,

$$C_V(T, \mathbf{H}) = T \left(\frac{\partial S}{\partial T} \right)_{H, V}. \quad (6)$$

At low T and H , when the gap varies weakly with temperature, the temperature derivative acts only on the Fermi function in Eq.(5), and the specific heat is given by the simple form

$$C_V(T, \mathbf{H}) \approx \frac{1}{2} \int_{-\infty}^{\infty} d\omega N(\omega, \mathbf{H}) \frac{\omega^2}{T^2} \text{sech}^2 \frac{\omega}{2T}. \quad (7)$$

Here we consider the full range of temperatures below the transition, and hence evaluate the specific heat from Eq. (6). We approximate the temperature dependence of the order parameter, $\Delta_{\mathbf{k}}(T)$, according to the BCS weak-coupling ansatz appropriate to a circular Fermi surface³⁵

$$\Delta(T) = \Delta_0 \cos(2\phi) \tanh \left(\frac{\pi T_c}{\Delta_0} \sqrt{\frac{4}{3} \frac{8}{7\zeta(3)} \left(\frac{T_c}{T} - 1 \right)} \right), \quad (8)$$

where $\Delta_0 = 2.14T_c$ is the gap maximum.

In the absence of impurity scattering, there are two important low energy energy scales in the problem: the temperature T and the magnetic energy, or typical Doppler shift $E_H \equiv v_F/R_H$. To satisfy the requirements of the semiclassical approach, we consider only $E_H \ll \Delta_0$, but temperature to vary over the entire range $T < T_c$.

III. DENSITY OF STATES IN PLANAR FIELD

In the nodal approximation of Ref. 3, the quasiparticle momentum \mathbf{k} is replaced by its value \mathbf{k}_n at each of the 4 nodes, which are then summed over. The residual density of states at the Fermi level, Eq. (4) then becomes

$$\frac{N(0, \mathbf{H})}{N_0} = \frac{2\sqrt{2}}{\pi} \frac{E_H}{\Delta_0} \beta(\theta), \quad (9)$$

where the angular variation is given by $\beta(\theta) = \max(|\sin \theta|, |\cos \theta|)$. Eq. (7) then yields the linear in temperature specific heat at low T with the slope

$$\lim_{T \rightarrow 0} \frac{C_V(T; \mathbf{H})}{T} \simeq \frac{4\sqrt{2}\pi}{3} \frac{E_H}{\Delta_0} \beta(\theta). \quad (10)$$

At low energies, $E_H, \omega \ll \Delta_0$, the density of states in the nodal approximation with linearized order parameter takes the form^{3,6}

$$\frac{N(\omega, \mathbf{H}, T)}{N_0} = \frac{1}{2} \left[\frac{E_1}{\Delta_0} F\left(\frac{\omega}{E_1}\right) + \frac{E_2}{\Delta_0} F\left(\frac{\omega}{E_2}\right) \right], \quad (11)$$

where $E_1 = E_H |\sin(\pi/4 - \theta)|$, $E_2 = E_H |\cos(\pi/4 - \theta)|$, and the scaling function F is given by⁵

$$F(y) = \begin{cases} y [1 + 1/(2y^2)], & \text{if } y \geq 1; \\ \left[(1 + 2y^2) \arcsin y + 3y\sqrt{1-y^2} \right] / y\pi, & \text{if } y \leq 1. \end{cases} \quad (12)$$

Note that in the limit $y \rightarrow \infty$, $F(y) \rightarrow y$, such that $N(\omega, \mathbf{H}, T)$ in (4) recovers the *isotropic* low- ω d -wave density of states ω/Δ_0 . Thus in the nodal approximation with linearized order parameter the specific heat oscillations are washed out at higher temperatures, but the method cannot generate specific heat oscillation inversions.

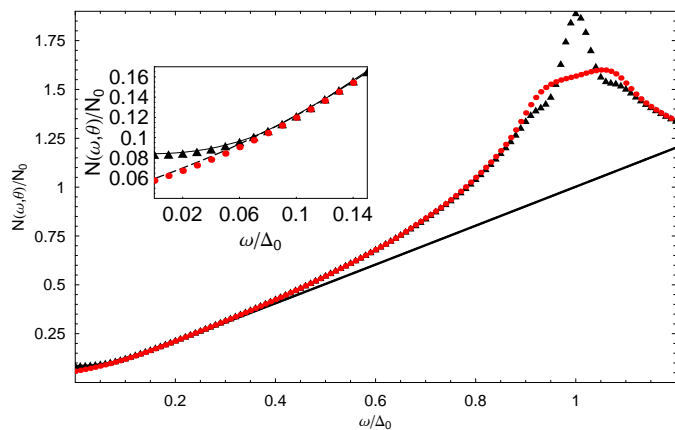


FIG. 1: (Color online) Comparison of the nodal approximation Eq.(11) for the density of states $N(\omega, \mathbf{H})$ versus the full density of states at $T = 0.001T_c$ and $E_H = 0.2T_c$. solid line: nodal approximation for \mathbf{H} along antinode. Dashed line: nodal approximation for \mathbf{H} along node. Red circles: full evaluation for \mathbf{H} along node. Black triangles: full evaluation for \mathbf{H} along antinode. The insert magnifies the low-frequency range.

In Fig. 1, we now compare the density of states of a d -wave superconductor obtained from a complete evaluation of Eq. (4) with the nodal approximation with linearized order parameter Eq. 11. In agreement with all previous work the density of states for field in nodal and antinodal directions is strongly anisotropic for $\omega \lesssim E_H$, and the anisotropy is washed out at higher energies. However, the difference between $N(\omega, \mathbf{H}, T)$ for the two directions of the field reappears at energies of order Δ_0 , the energy scale absent in the versions of the calculation with linearized gap.

For the field along the antinode $\mathbf{H} \parallel \mathbf{k}_{an}$ ($\theta = 0, \pi/2, \dots$) the density of states continues to be sharply peaked at Δ_0 , as in the absence of the field. This peak is largely

due to the quasiparticles moving along the field, which do not experience the Doppler shift and see the full maximal gap. In contrast, for the field along the node, $\mathbf{H} \parallel \mathbf{k}_n$ ($\theta = \pi/4, 3\pi/4, \dots$), the DOS has broad features around $\Delta_0 \pm E_H$. As a result, the density of states for the field along the nodal direction begins to exceed that for field along the antinode at the lower shoulder, and the DOS anisotropy is inverted, relative to that at low energies.

We emphasize that the absence of the structure near the gap edge in $N(\omega, \mathbf{H}, T)$ in previous work is a consequence of gap linearization, and not the nodal approximation. We observe features similar to those depicted in Fig. 1 when replacing $\mathbf{k} \rightarrow \mathbf{k}_n$ in the Doppler shift, but keeping the full variation of the order parameter around the Fermi surface. Of course, the nodal approximation is not accurate at the energies of order Δ_0 , and hence we continue with the full evaluation of the DOS.

The anisotropy in the density of states that we computed differs from that found in Refs.^{17,18}, where noticeable inversion of the anisotropy in $N(\omega, \mathbf{H}, T)$ occurred already at relatively low energy, as a result of the competition between Doppler shift and vortex scattering. Remarkably, we find that even within the semiclassical method, when the lifetime remains infinite and the scattering on the vortices is neglected, the anisotropy in the density of state is still reversed, albeit at higher energies of order of the gap maximum.

The possibility of an inversion of the specific heat anisotropy is clear from Fig. 1. In Eq. (7) the density of states is convoluted with the temperature-dependent weighting function, peaked around $\omega \simeq 2.5T$. At a given field, as the temperature is increased, more weight in the kernel shifts to higher energies, where the anisotropy in the DOS is opposite to that at low ω . Whether an inversion then occurs at higher T depends primarily on whether the kernel has sufficient weight in the exponential tail at energies $\omega \simeq \Delta_0 - E_H$. Since the DOS anisotropy is small in magnitude above this crossing energy, the specific heat must be calculated numerically.

In Figure 2 we plot the density of states as a field sweeps through the ab-plane. We clearly see that for low frequency the node and minimum in the oscillations coincide, and that at higher frequencies this is no longer the case. The eventual inversion of this pattern results in the angular density of states having a maximum at the gap node for higher frequencies.

IV. SPECIFIC HEAT OSCILLATIONS

Numerical differentiation of the entropy is computationally intensive due to the high accuracy required in finding S in Eq. (5). To illustrate the precision of our calculations in Fig. 3, we show the numerically evaluated specific heat at $H = 0$ and at $E_H = 0.4T_c$ for the field along the a-axis over a wide temperature range both below and above T_c . The normal state specific heat above T_c is $C_N = \gamma_N T \equiv 2N_0\pi^2T/3$, where N_0 is the Fermi

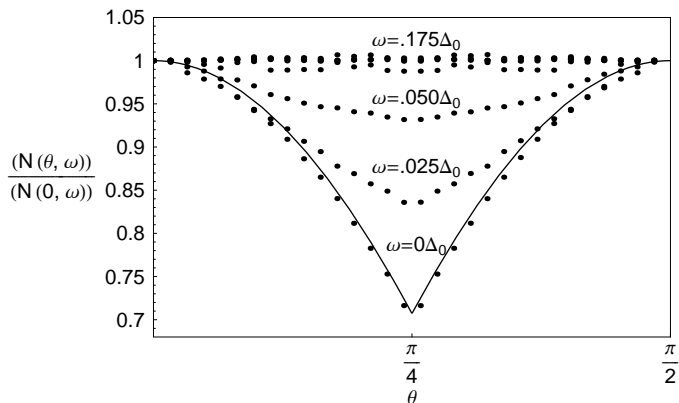


FIG. 2: DOS $N(\theta, \omega)$ vs. magnetic field angle θ at $E_h = 0.2T_c$ and $T = 0.05T_c$ for equally spaced frequencies, $0.025\Delta_0$ apart, from $\omega = 0$ to $0.175\Delta_0$. The solid line is the result of the nodal approximation for the $\omega = 0$ DOS from Eq. (9).

level DOS per spin.

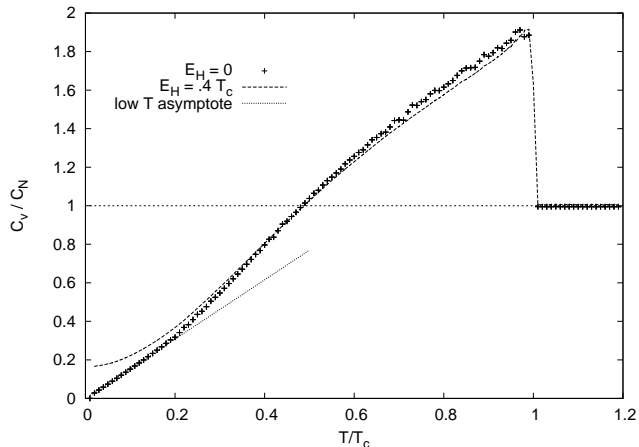


FIG. 3: Temperature dependence of the specific heat (at constant volume) normalized to the specific heat in the normal state C_V/C_N , where $C_N = \gamma_N T$. We show both the exact (symbols), and the asymptotic low- T (dotted line) behavior in the absence of the field, and compare it to the numerically determined C_V/C_N at $E_H = 0.4T_c$ (dashed line). There is no reduction of T_c with field in our approach.

To test our numerical evaluations we first check the numerical results against the asymptotic low-temperature specific heat in zero field. For our model of a 2D d -wave superconductor with a circular Fermi surface at $T \ll T_c$ we find

$$\frac{C_V}{N_0 T} \approx \gamma_0 \frac{T}{T_c}, \quad (13)$$

$$\gamma_0 = \frac{T_c}{\Delta_0} \int_0^\infty \frac{x^3 dx}{\cosh^2(x/2)} = \frac{T_c}{\Delta_0} 18\zeta(3) \approx 10.11, \quad (14)$$

which agrees with the numerically determined slope. The Volovik effect is manifested in Fig. 3 in the finite offset

of C/T (Eq. (10) in the presence of magnetic field $E_H = 0.4T_c$.

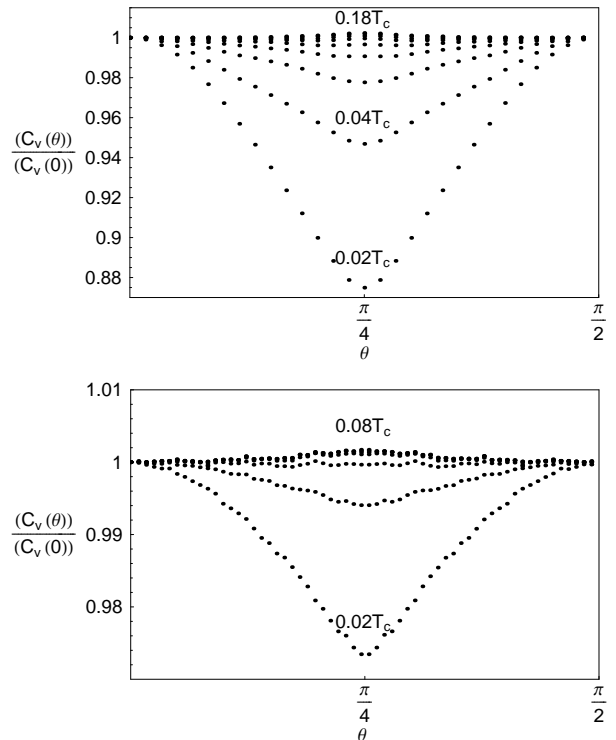


FIG. 4: Upper panel: $C(T, \mathbf{H})/C(T, \theta = \mathbf{0})$ vs. θ for a set of equally spaced temperatures, every $0.02T_c$, from 0 to $0.18T_c$, $E_h = 0.2T_c$. Lower panel: same for a set of equally spaced temperatures from 0 to $0.08T_c$ every $0.02T_c$, $E_h = 0.05T_c$.

We proceed to evaluate the specific heat for fixed E_H and several temperatures as a function of the field angle θ . Fig. 4 shows that the inversion of the DOS anisotropy found in Sec. III indeed are sufficient to lead to the inversion of the specific heat oscillations a characteristic temperature, T_{inv} . In Fig. 4 the fourfold oscillations are clearly visible at low T , and minima occur for \mathbf{H} along nodal directions as anticipated. However, at higher temperatures, an inversion in the pattern of oscillations is evident. In Fig. 5 we examine the anisotropy by plotting the difference between the specific heat for the field along the nodal and the antinodal directions, which identifies the temperature at which inversion occurs.

Since in our approach the inversion is due to the sensitivity of the specific heat to the changes in the DOS within energy range $\sim E_H$ of the gap edge, increasing both the magnetic field and the temperature initially enhances the amplitude of the inverted oscillations. Increasing the field brings the anisotropy inversion down in energy in Fig. 1; raising the temperature increases the contribution of the high energy regions in C/T . While the amplitude of the inverted (relative to those at $T = 0$) oscillations in C_V is small, it is of the same order of magnitude as that observed experimentally^{7,9-12}, and found theoretically for a quasi-two-dimensional system at mod-

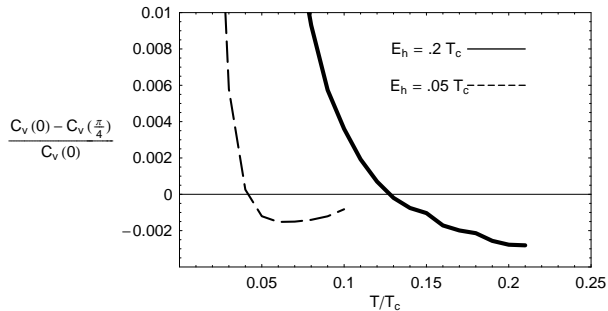


FIG. 5: Amplitude of specific heat oscillation defined by difference of C_V between node and antinode, $[C_V(0) - C_V(\frac{\pi}{4})]/C_V(0)$ for $E_H = 0.2T_c$ (solid line) and $E_H = 0.05T_c$ (dashed line).

erate fields^{17,18}. Of course, when H (T) approaches the upper critical field (the transition temperature) respectively, the gap in the spectrum closes, and the oscillations vanish; we cannot, however, reliably comment on the evolution of the anisotropy in this regime within the semiclassical method. At the same time it follows from our analysis that the amplitude of the inverted oscillations has a maximum at intermediate fields and temperatures, also in agreement with Refs.^{17,18}. Therefore our results connect well with those obtained by a different technique.

V. CONCLUSIONS

In this paper we have calculated the specific heat of a two-dimensional d -wave superconductor in an external magnetic field using the semiclassical treatment of the effect of the vortex lattice on the quasiparticle spectrum. In contrast to previous work utilizing the nodal approximation with linearized order parameter, we carried out a full numerical evaluation of the density of states and the entropy for a wide range of fields and temperatures. Our main finding is that the *sign* of the oscillations of the specific heat as a function of the field orientation, i.e. the difference between C_V for the field along a nodal direction and along the antinode, depends on the temperature and field strength. We confirmed that at low temperatures and fields the specific heat has a minimum when the field is along a nodal direction. However, as H and T are increased, minima of the specific heat begin to occur for the field along the gap maxima, i.e. an inversion of the oscillation pattern occurs. Note that while we considered a system with well-defined quasiparticle states, it is reasonable to believe that scattering due to impurities or vortex lattice disorder will merely smear the anisotropy on both sides of the inversion line.

Our calculations provide a bridge connecting the semiclassical theory at low fields $H \ll H_{c2}$ with the results of the extended Brandt-Pesch-Tewordt approxima-

tion^{17,18}, where the inversion was first found. The latter approach is in principle valid at $H \lesssim H_{c2}$, but has been shown to provide remarkably good agreement with semiclassical predictions down to low fields, up to log corrections¹⁸. To compare the results of the two approaches explicitly, we extend our calculation to higher fields, account for the field dependence of the gap amplitude via $\Delta(T, H) = \Delta(T)\sqrt{1 - H/H_{c2}}$, and determine the inversion line. This provides a direct comparison with the results of Ref. 18, where the same field dependence was assumed for a circular Fermi surface identical to that considered above. In Fig. 6 we plot the approximate crossover scales for both the Brandt-Pesch-Tewordt and semiclassical theories. There is a remarkably good qualitative agreement for the behavior of the inversion line up to moderate fields, where the ranges of validity of the two approaches may reasonably be assumed to overlap. This establishes a phase diagram for when the specific heat is expected to have minima or maxima at the gap nodes. Taken together, these results strongly suggest that the

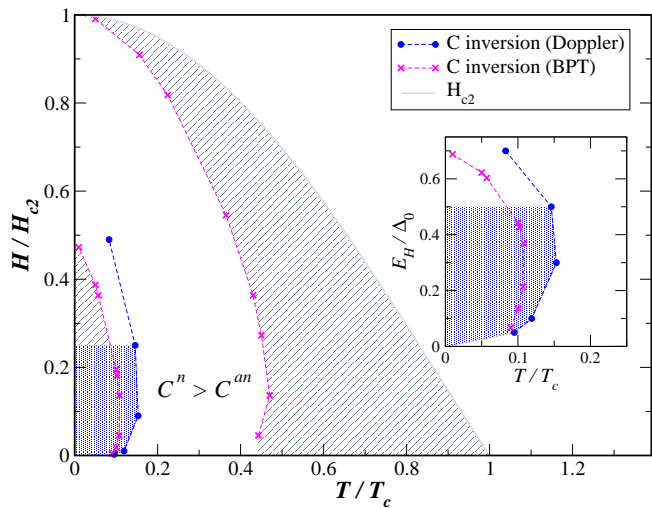


FIG. 6: Phase diagram H/H_{c2} vs. T/T_c for specific heat oscillations of a d -wave superconductor in a magnetic field. The shaded regions indicate that the specific heat $C(T, \mathbf{H})$ has a minimum when the field \mathbf{H} points in the nodal direction, whereas the white regions indicate inverted oscillations, where minima correspond to field along antinode. The gray shaded regions are results from Ref. 18 using the Brandt-Pesch-Tewordt framework, whereas the blue regions represent the region of the $H - T$ plane where minima correspond to nodes within the semiclassical theory. The phase diagram comparing both approaches was determined using the assumption $H/H_{c2} = (E_H/\Delta_0)^2$, valid up to a prefactor of order unity. Insert: blowup of the low T and H region. Note the field scale is given in terms of E_H/Δ_0 for easier comparison with other results in this work.

inversion of the specific heat oscillations with temperature is a general feature for all nodal superconductors, and establish the approximate location of the inversion line.

Consequently, identification of the nodes in the gap

via the specific heat measurements is not as straightforward as the original semiclassical results suggested, and depends on where the experiment is done in the field-temperature plane. While the inversion of the oscillations in related experiments on the anisotropy of the heat conductivity of nodal superconductors has been well established^{15,36–38}, an inversion in the heat capacity measurements has not yet been searched for systematically. Experimental identification of the inversion line in the T - H plane would be an important step towards further establishing the heat capacity measurements as the method of choice for determining the nodal directions in the bulk, and our paper provides theoretical foundation for such a

search.

Acknowledgments

This work was supported in part by DOE DE-FG02-05ER46236 (P.J.H. and G.R.B.), the Louisiana Board of Regents (I.V. and A.B.V.), and DOE DE-FG02-08ER46492 (I. V.). This work was started at the Institut d'Études Scientifiques de Cargèse, and supported there in part by the I2CAM via NSF grant DMR 0645461. GRB and PJH acknowledge useful discussions with S. Graser.

-
- * Present address: Dept. of Physics, University of Wisconsin, Madison, WI
- ¹ N. Hussey, *Adv. Phys.* **51**, 1685 (2002).
 - ² C. C. Tsuei and J. R. Kirtley, *Rev. Mod. Phys.* **92**, 969 (2000).
 - ³ I. Vekhter, P. J. Hirschfeld, E. J. Nicol, and J. P. Carbotte, *Phys. Rev. B* **59**, R9023 (1999).
 - ⁴ G. E. Volovik, *JETP Letters* **58**, 469 (1993).
 - ⁵ C. Kübert and P. J. Hirschfeld, *Solid State Commun.* **105**, 459 (1998).
 - ⁶ I. Vekhter, P. Hirschfeld, and E. Nicol, *Phys. Rev. B* **64**, 064513 (2001).
 - ⁷ T. Park, M. B. Salamon, E. M. Choi, H. J. Kim, and S.-I. Lee, *Phys. Rev. Lett.* **90**, 177001 (pages 4) (2003).
 - ⁸ T. Park and M. B. Salamon, *Mod. Phys. Lett. B* **18**, 1205 (2004).
 - ⁹ H. Aoki, T. Sakakibara, H. Shishido, R. Settai, Y. Onuki, P. Miranović, and K. Machida, *Journal of Physics: Condensed Matter* **16**, L13 (2004).
 - ¹⁰ K. Deguchi, Z. Q. Mao, H. Yaguchi, and Y. Maeno, *Phys. Rev. Lett.* **92**, 047002 (2004).
 - ¹¹ T. Sakakibara, A. Yamada, J. Custers, K. Yano, T. Tayama, H. Aoki, and K. Machida, *J. Phys. Soc. Jpn* **76**, 051004 (2007).
 - ¹² K. Yano, T. Sakakibara, T. Tayama, M. Yokoyama, H. Amitsuka, Y. Homma, P. Miranović, M. Ichioka, Y. Tsutsumi, and K. Machida, *Phys. Rev. Lett.* **100**, 017004 (2008).
 - ¹³ K. Deguchi, Z. Q. Mao, H. Yaguchi, and Y. Maeno, *J. Phys. Soc. Jpn* **73**, 1313 (2004).
 - ¹⁴ K. Izawa, H. Yamaguchi, Y. Matsuda, H. Shishido, R. Settai, and Y. Onuki, *Phys. Rev. Lett.* **87**, 057002 (2001).
 - ¹⁵ Y. Matsuda, K. Izawa, and I. Vekhter, *J. Phys.: Cond. Mat* **18**, R705 (2006).
 - ¹⁶ M. Udagawa, Y. Yanase, and M. Ogata, *Phys. Rev. B* **70**, 184515 (2004).
 - ¹⁷ A. Vorontsov and I. Vekhter, *Phys. Rev. Lett.* **96**, 237001 (2006).
 - ¹⁸ A. B. Vorontsov and I. Vekhter, *Phys. Rev. B* **75**, 224501 (2007).
 - ¹⁹ U. Brandt, W. Pesch, and L. Tewordt, *Z. Phys.* **201**, 209 (1967).
 - ²⁰ W. Pesch, *Z. Phys. B* **21**, 263 (1975).
 - ²¹ G. E. Volovik, unpublished; in K. A. Moler *et al.*, *J. Phys. Chem. Solids* **56**, 1899 (1995).
 - ²² Y. Wang, B. Revaz, A. Erb, and A. Junod, *Phys. Rev. B* **63**, 094508 (2001).
 - ²³ K. A. Moler, D. J. Baar, J. S. Urbach, R. Liang, W. N. Hardy, and A. Kapitulnik, *Phys. Rev. Lett.* **73**, 2744 (1994).
 - ²⁴ K. A. Moler, D. S. Sisson, J. S. Urbach, M. R. Beasley, A. Kapitulnik, D. J. Baar, R. Liang, and W. N. Hardy, *Phys. Rev. B* **55**, 3954 (1997).
 - ²⁵ C. Kübert and P. J. Hirschfeld, *Phys. Rev. Lett.* **80**, 4963 (1998).
 - ²⁶ M. Franz and Z. Tešanović, *Phys. Rev. Lett.* **84**, 554 (2000).
 - ²⁷ D. Knapp, C. Kallin, and A. J. Berlinsky, *Phys. Rev. B* **64**, 014502 (2001).
 - ²⁸ D. Knapp, C. Kallin, and A. J. Berlinsky, *Phys. Rev. B* **64**, 149902(E) (2001).
 - ²⁹ T. Dahm, S. Graser, C. Iniotakis, and N. Schopohl, *Phys. Rev. B* **66**, 144515 (2002).
 - ³⁰ R. Movshovich, M. Jaime, J.D. Thompson, C. Petrovic, Z. Fisk, J. Pagliuso, and J.L. Sarrao, *Phys. Rev. Lett.* **86**, 5152 (2001).
 - ³¹ Y. Kamihara, T. Watanabe, M. Hirano, and H. Hosono, *J. Am. Chem. Soc.* **130**, 3296 (2008).
 - ³² J. Clem, M.W. Coffey, *Phys. Rev. B* **42**, 6209 (1990).
 - ³³ S. Graser, G. Boyd, C. Cao, H.P. Cheng, P.J. Hirschfeld, D.J. Scalapino, *Phys. Rev. B Rapid Communications* submitted. arXiv:0804.0887
 - ³⁴ Y. Tanaka, K. Kuroki, Y. Tanuma, and S. Kashiwaya, *J. Phys. Soc. Jpn* **72**, 2157 (2003).
 - ³⁵ D. Einzel, *J. Low Temp. Phys.* **131**, 1 (2003).
 - ³⁶ H. Aubin, K. Behnia, M. Ribault, R. Gagnon, and L. Taillefer, *Phys. Rev. Lett.* **78**, 2624 (1997).
 - ³⁷ T. Watanabe, K. Izawa, Y. Kasahara, Y. Haga, Y. Onuki, P. Thalmeier, K. Maki, and Y. Matsuda, *Phys. Rev. B* **70**, 184502 (2004).
 - ³⁸ Y. Kasahara, T. Iwasawa, Y. Shimizu, H. Shishido, T. Shibauchi, I. Vekhter, and Y. Matsuda, *Phys. Rev. Lett.* **100**, 207003 (2008).